Fluctuations and response in a non-equilibrium micron-sized system

Juan Ruben Gomez-Solano, Artyom Petrosyan, Sergio Ciliberto, Christian

Maes

▶ To cite this version:

HAL Id: ensl-00492526

https://ens-lyon.hal.science/ensl-00492526v3

Submitted on 30 Nov 2010

Fluctuations and response in a non-equilibrium micron-sized system

Juan Ruben Gomez-Solano[1], Artyom Petrosyan[1], Sergio Ciliberto[1] and Christian Maes[2]
Email: juan.gomez_solano@ens-lyon.fr, artyom.petrosyan@ens-lyon.fr,
sergio.ciliberto@ens-lyon.fr and christian.maes@fys.kuleuven.be
[1]Laboratoire de Physique, Ecole Normale Supérieure de Lyon, CNRS UMR 5672,
46, Allée d'Italie, 69364 Lyon CEDEX 07, France
[2]Instituut voor Theoretische Fysica, K. U. Leuven, B-3001 Leuven, Belgium

November 30, 2010

Abstract

The linear response of non-equilibrium systems with Markovian dynamics satisfies a generalized fluctuation-dissipation relation derived from time symmetry and antisymmetry properties of the fluctuations. The relation involves the sum of two correlation functions of the observable of interest: one with the entropy excess and the second with the excess of dynamical activity with respect to the unperturbed process, without recourse to anything but the dynamics of the system. We illustrate this approach in the experimental determination of the linear response of the potential energy of a Brownian particle in a toroidal optical trap. The overdamped particle motion is effectively confined to a circle, undergoing a periodic potential and driven out of equilibrium by a non-conservative force. Independent direct and indirect measurements of the linear response around a non-equilibrium steady state are performed in this simple experimental system. The same ideas are applicable to the measurement of the response of more general non-equilibrium micron-sized systems immersed in Newtonian fluids either in stationary or non-stationary states and possibly including inertial degrees of freedom.

1 Introduction

The linear response of systems in thermodynamic equilibrium is generally described by the fluctuation-dissipation theorem [1]. It provides a simple relation between the equilibrium fluctuations of an observable Q with the response due to a small external perturbation h_s changing the potential at time s as $U \to U - h_s V$:

$$R_{QV}(t-s) = \beta \frac{\mathrm{d}}{\mathrm{d}s} \langle Q(t) V(s) \rangle_0. \tag{1}$$

In equation (1) $R_{QV}(t-s) = \delta \langle Q(t) \rangle_h / \delta h_s |_{h=0}$ is the linear response function of Q at time $t \geq s$; $\langle Q(t) V(s) \rangle_0$ is the two-time correlation function between Q and V measured at equilibrium; the brackets $\langle \ldots \rangle_h$ denote the ensemble average in the state perturbed by h_s so that $\langle \ldots \rangle_0$ corresponds to the ensemble average at equilibrium ($h_s = 0$). The inverse temperature of the equilibrium system, $\beta = 1/k_B T$, appears as a multiplicative factor. Hence, equation (1) represents a useful tool in experiments and simulations to explore indirectly the linear response regime from fluctuation measurement completely performed at thermal equilibrium. Vice versa,

one can obtain information on microscopic fluctuations from non-equilibrium measurements of response functions or susceptibilities by applying sufficiently weak external fields.

In general, equation (1) fails to describe the linear response of systems already prepared in a non-equilibrium state. This situation is relevant in real mesoscopic systems that usually operate far from equilibrium due to either non-conservative/time-dependent forces exerted by the experimental apparatus or external flows and gradients applied at the boundaries. For instance, the developement of micro and nano techniques (*e.g.* optical tweezers and atomic force microscopes) has allowed one to mechanically manipulate colloidal particles, living cells and single molecules of biological interest with forces ranging from pN to fN. In this kind of experiments, thermal fluctuations can be comparable or larger than the typical external perturbations necessary to determine R_{QV}. Then, for these systems it is more reliable in practice to measure non-equilibrium fluctuations than linear response functions.

On the theoretical side, several works have recently dealt with the problem of the extension of the fluctuation-dissipation theorem around non-equilibrium steady states [2, 3, 4, 5, 6, 7, 8, 9, 10, 11]. In most of the formulations, an additive extra term on the right-hand side of equation (1) appears as a non-equilibrium correction of the fluctuation-dissipation relation due to the broken detailed balance. Different physical interpretations of the corrective term are provided in the literature. We specially highlight the roles of the non-vanishing probability current [6] and the conjugate variables to the total entropy production [5, 11] in the analytical expression of the corrective term, leading independently to a Lagrangian interpretation for Langevin systems with first-order Markovian dynamics. Following these two approaches an equilibrium-like fluctuation-dissipation relation can be restored in the Lagrangian frame of the local mean velocity of the system for the right choice of observables [5, 6, 12]. An alternative interpretation, the *entropic-frenetic* approach, has been proposed in terms of time-symmetric and time-antisymmetric properties of the fluctuations [13, 14, 15]. Unlike previous formulations, the entropic-frenetic approach does not involve the stationary probability distribution of the degree of freedom of interest but only explicit observables. In addition, it holds even in more general situations including non-steady states and inertial degrees of freedom provided that the dynamics is Markovian [15]. Therefore it is more accessible from the experimental point of view.

The present paper provides the first experimental investigation of the modified fluctuation-response relation of [13, 14] in a simple experimental system driven into a non-equilibrium steady state: a Brownian particle whose overdamped motion is effectively confined to a circle by a toroidal optical trap [16]. As the new formula relating response and fluctuations is exact and does not involve further notions such as effective temperatures, it can be tested at full value. Moreover, we do not need the explicit knowledge (analytic form) of the stationary distribution. Hence the experimental linear response of the system can be safely determined by two independent methods. In the first method one control parameter of the non-equilibrium steady state is physically perturbed and the corresponding response of the particle is directly measured. In the second method, only the unperturbed non-equilibrium fluctuations of the position of the particle are measured and the same linear response is determined based on the generalized fluctuation-dissipation formula and on a suitable model of the dynamics. All of this is done here under very well controlled experimental conditions, so that all can be checked explicitly and every step can be analyzed separately. That control allows us to understand the usefulness of the new formalism so that it will be able to be employed also in natural situations where such a control is really absent, and *e.g.* the driving or potential are not exactly known.

The paper is organized as follows: in section 2 we briefly present the generalized approach to linear response based on the entropic-frenetic formulation of a fluctuation-dissipation relation for systems with Markovian dynamics and the main goals of our experimental study with respect to this formalism. In section 3 we describe the main features of the experiment and the 1D Langevin model of the translational motion of the particle in the toroidal trap. In section 4

we present the results of the two methods to measure the linear response function of the system. We show that within our experimental accuracy both methods lead to the same values of the linear response function when taking into account the corrections given by the generalized fluctuation-dissipation relation. Then, we discuss their technical limitations and advantages from the experimental point of view. We also depict a simple example in order to show the flexibility of the generalized fluctuation-dissipation formula: once the unperturbed fluctuations of the proper degree of freedom are measured, one can readily compute the linear response of the system under more complex time-dependent perturbations. Finally we present the conclusion.

2 Generalized approach to linear response

We briefly present the formulation of the fluctuation-dissipation relation developed in [13, 14, 15] for the special case of stochastic systems described by a finite number of degrees of freedom $\{q\}$ with overdamped Markovian Langevin dynamics, in presence of a potential $U(q)$. We consider a system in contact with a thermal bath at temperature T and driven into a non-equilibrium steady state by a non-conservative force. We focus on the average value of an observable $Q(q)$ at time t, denoted by $\langle Q(q_t) \rangle_0$. We are also interested in the mean value $\langle Q(q_t) \rangle_h$ of $Q(q)$, when a small time dependent perturbation h_s is applied to $U(q)$, namely $U(q) \to U(q) - h_s V(q)$. As formally shown in [13, 14], $\langle Q(q_t) \rangle_h$ is given at linear order in h_s by

$$\langle Q(q_t) \rangle_h = \langle Q(q_t) \rangle_0 + \int_{-\infty}^{t} R_{QV}(t,s) h_s \, \mathrm{d}s, \tag{2}$$

where the linear response function R_{QV} obeys the generalized fluctuation-dissipation relation

$$R_{QV}(t,s) = \frac{\beta}{2} \frac{\mathrm{d}}{\mathrm{d}s} \langle V(q_s) Q(q_t) \rangle_0 - \frac{\beta}{2} \langle LV(q_s) Q(q_t) \rangle_0. \tag{3}$$

In equation (3), L is the generator of the unperturbed Langevin dynamics which determines the time evolution of any single-time observable $O(q)$: $\mathrm{d}\langle O(q_t) \rangle_0 / \mathrm{d}t = \langle (LO)(q_t) \rangle_0$.

It should be noted that $R_{QV}(t,s)$ is operationally obtained by applying an instantaneous delta perturbation at time s and measuring $\langle Q(q_t) \rangle_h - \langle Q(q_t) \rangle_0$. In experiments it is always more reliable to apply a Heaviside perturbation ($h_s = 0$ for $s < 0$, $h_s = h = const.$ for $s \geq 0$) instead. This procedure directly yields the integrated response function

$$\chi_{QV}(t) = \int_0^t R_{QV}(t,s) \, \mathrm{d}s = \frac{\langle Q(q_t) \rangle_h - \langle Q(q_t) \rangle_0}{h}, \tag{4}$$

defined over the time interval $[0, t]$. Therefore, in the following we consider the integral form of equation (3)

$$\chi_{QV}(t) = \frac{\beta}{2} [C(t) + K(t)], \tag{5}$$

where the term

$$C(t) = \langle V(q_t) Q(q_t) \rangle_0 - \langle V(q_0) Q(q_t) \rangle_0, \tag{6}$$

can be interpreted as a correlation between the observable $Q(q_t)$ and the excess in entropy produced by the Heaviside perturbation during the interval $[0, t]$: $[hV(q_t) - hV(q_0)]/T$. On the other hand, the term

$$K(t) = - \int_0^t \langle LV(q_s) Q(q_t) \rangle_0 \, \mathrm{d}s, \tag{7}$$

can be interpreted as minus the correlation between $Q(q_t)$ and the integrated excess in dynamical activity or *frenesy*: $\beta \int_0^t LV(q_s) h \mathrm{d}s$, which quantifies how frenetic the motion is due to the

3

perturbation with respect to the unperturbed process. The frenesy $\beta LV(q)$ can be regarded as a generalized escape rate of a trajectory from a given phase-space point q. In references [13, 14, 15] it has been widely discussed that the origin of the entropic $C(t)$ and the frenetic $K(t)$ terms can be traced back to time-antisymmetric and symmetric properties of the fluctuations, respectively.

The non-equilibrium fluctuation-response formulae (3) and (5) result directly from the theory of the Langevin equation, and hence, the validity of a Langevin model for our experiment would thus also imply this particular fluctuation-response formula. Since for the present experiment the Langevin equation has been largely verified before, thus implying in theory the response (2)-(7), the point of the present experimental study is not in the very first place to validate (2)-(7), although we still want to make sure it is exact. Rather, the point of the present investigation is much more twofold:

1) to show how the (very new) frenetic term (7) can indeed be measured independently and directly, without recourse to anything but the dynamics. In particular, no knowledge of the analytical expression of the stationary distribution is used;

2) to show how the new formalism (2)-(7) of response can be used to determine unknown forces, both conservative and non-conservative. For example, when the formula is accepted as such, the correction to the equilibrium formula gives useful information about how the breaking of detailed balance gets established. Alternatively, by changing the driving we can discover the potential that acts on the particle, etc.

These points are addressed in the following sections under proper experimental control and data analysis, which allows us to understand how the generalized fluctuation-response formalism can be applied to a real non-equilibrium experiment.

3   Colloidal particle in a toroidal optical trap

3.1   Experimental description

We specifically study the linear response of a single colloidal particle driven out of equilibrium by a non-conservative force in presence of a non-linear potential. We recall the main features of the experiment, previously described in detail in reference [16], where the same experimental set-up was used in the context of a modified fluctuation-dissipation relation with a different interpretation from the one described in the present paper. In our experiment the Brownian motion of a spherical silica particle (radius $r = 1\,\mu$m) immersed in water is confined on a thin torus of major radius $a = 4.12\,\mu$m by a tightly focused laser beam rotating at 200 Hz (see figure 1(a)). The rotation frequency of the laser is so high that it is not able to trap continuously the particle in the focus because the viscous drag force of the surrounding water quickly exceeds the optical trapping force. Consequently, at each rotation the beam only kicks the particle a small distance along the circle of radius a. During the absence of the beam ($\approx$ 5 ms), the particle undergoes free diffusion of less than 40 nm in the radial and perpendicular direction to the circle. Thus, the particle motion is effectively confined on a circle: the angular position θ of its barycenter is the only relevant degree of freedom of the dynamics. In addition, a static light intensity profile is created along the circle by sinusoidally modulating in time the laser power which has a mean value of 30 mW and a modulation amplitude of 4.2 mWpp at the same frequency as the rotation frequency of the beam. Figure 1(a) sketches this experimental configuration on a snapshot of the colloidal particle in the toroidal trap. The water reservoir acts as a thermal bath at fixed temperature ($T = 20 \pm 0.5°$C) providing thermal fluctuations to the particle. The viscous drag coefficient at this temperature is $\gamma = 1.89 \times 10^{-8}$ kg s^{-1}.
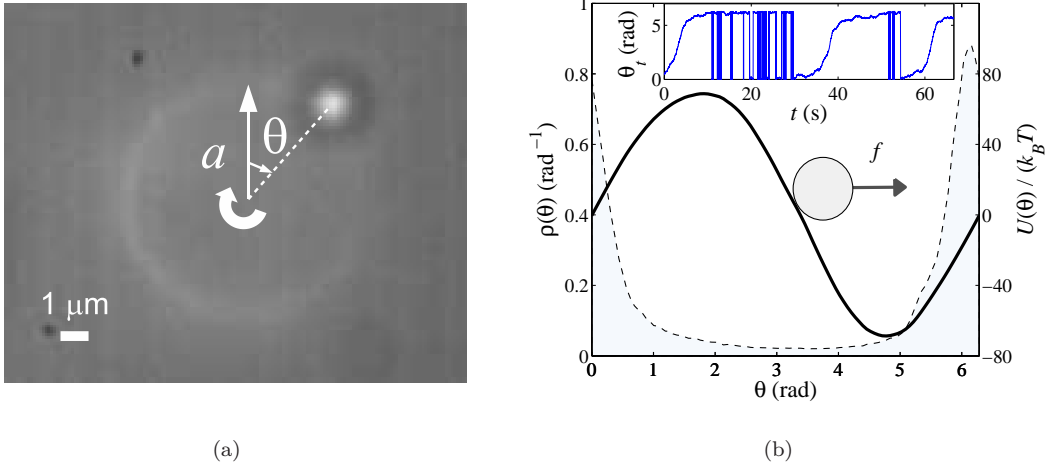
Figure 1: (a) Snapshot of the colloidal particle in the toroidal optical trap. The vertical arrow indicates the position $\theta = 0$ whereas the curled arrow shows the direction of the rotation of the laser beam. (b) Experimental potential profile (solid line) and probability density function of θ (dashed line) for the non-equilibrium steady state generated by the non-conservative force f. Inset: Typical steady-state trajectory $\{\theta_t,\ 0 \leq t \leq 66.67\ \mathrm{s}\}$ used to compute $\rho(\theta)$.

3.2   Model

For the experimentally accessible length and time scales the dynamics of θ is modeled by the first-order Langevin equation

$$\dot{\theta} = -A\phi'(\theta) + F + \xi, \tag{8}$$

as extensively verified in [16, 17, 18, 19, 20]. $A\phi(\theta)$ is a periodic non-linear potential $[A\phi(\theta) = A\phi(\theta + 2\pi)]$ of amplitude $A = 0.87$ rad^2 s^{-1} created by the periodic modulation of the laser intensity. The normalized angular profile $\phi(\theta)$ of the potential $(\max\{|\phi(\theta)|\} = 1)$ is a slightly distorted sine function as a result of unavoidable experimental static defects of the toroidal optical trap (e.g. optical aberration). $F = 0.85$ rad s^{-1} is a constant force acting in the direction of the laser rotation which is associated to the mean kick of the beam. ξ is a white noise process of zero mean and covariance $\langle \xi_t \xi_s \rangle = 2D\delta(t-s)$ with bare diffusivity $D = k_B T/(\gamma a^2) = 1.26 \times 10^{-2}$ rad^2 s^{-1}, which models the thermal fluctuating force exerted by the water molecules. F is non-conservative $(\int_0^{2\pi} F d\theta = 2\pi F > 0)$ since the motion takes place on a circle, driving the system out of equilibrium. The physical non-conservative force and the potential are $f = \gamma a F = 66$ fN and $U(\theta) = \gamma a^2 A\phi(\theta) = 68.8 k_B T \phi(\theta)$, respectively. The experimental potential profile $U(\theta)$ is plotted as a continuous black line in figure 1(b). Note that at thermal equilibrium $(F = 0)$ the particle motion would be tightly confined around the potential minimum with the stochastic variable θ distributed according to the Boltzmann density $\rho_{eq}(\theta) \propto \exp[-\beta U(\theta)]$. However, due to the thermal fluctuations and the non-conservative force $F > 0$, the particle is able to go beyond the potential barrier and explore the whole circle. In the non-equilibrium situation with constant $F, A, D > 0$, the angular position θ settles in a stationary probability density $\rho(\theta) \neq \rho_{eq}(\theta)$ that admits an analytical expression found in [21]. The experimental non-equilibrium density $\rho(\theta)$ is shown in figure 1(b) as a dashed line. A constant probability current $j = \langle \dot{\theta}(t) \rangle_0/(2\pi) = [F - A\phi'(\theta)]\rho(\theta) - D\partial_\theta\rho(\theta) > 0$, in the direction of F appears reflecting the broken detailed balance of the dynamics. For the experimental conditions one finds $j = 3.76 \times 10^{-2}$ s^{-1} corresponding to a mean rotation period of 26.6 s for the particle.

5

Both $\rho(\theta)$ and j, determined from 200 independent experimental time series of the angular position of the particle $\{\theta_t,\, 0 \leq t \leq 66.67 \text{ s}\}$, allow one to precisely compute the values of f and $U(\theta)$, as described in detail in [16, 17]. One example of such a steady-state time series is depicted in the inset of figure 1(b).

4 Measurement of the linear response function around a non-equilibrium steady state

Now we proceed to determine the linear response of the particle motion when slightly perturbing the non-equilibrium steady state previously described. For experimental simplicity we consider a step perturbation to the potential amplitude $A \rightarrow A + \delta A$, so that the perturbation and its conjugate variable are $h = -\delta A$ and $V(q) = \phi(\theta)$, respectively. It should be noted that the dynamics of θ is strongly nonlinear as the particle undergoes the periodic potential $A\phi(\theta)$ but for sufficiently small values of δA the response of $\phi(\theta)$ can still be linear. In reference [16], where we used the same experimental data as in the present paper, we have already checked that for a perturbation δA of the potential amplitude A in the range $|\delta A| \leq 0.07A$ the linear response regime holds. This was done by computing the experimental integrated response $\chi(t)$ of the observable $Q(\theta) = \sin\theta$ for two different values of δA: $0.05A$ and $0.07A$. We showed that within the experimental error bars $\chi(t)$ is the same in both cases. The independence of $\chi(t)$ with respect to δA experimentally demonstrates that the system is actually in the linear response regime at least for $|\delta A| \leq 0.07A$ and times $0 \leq t \leq 3.3$ s after the application of the Heaviside perturbation.

In order to illustrate the meaning of the non-equilibrium linear response relation of equation (5) in this case, we perform two different kinds of independent measurements: *direct* and *indirect*, as explained in the following.

4.1 Direct measurement of the linear response function

First, we consider the *direct* measurement of the integrated response function χ_{QV} for the periodic observable $Q(q) = \phi(\theta) = \phi(\theta + 2\pi)$. This observable times $\gamma a^2 A$ represents the instantaneous potential energy of the particle. This is experimentally accomplished by applying a step perturbation to the amplitude of the sinusoidal laser power modulation, 4.2 mWpp $\rightarrow$ 4.4 mWpp, but keeping constant the power offset at 30 mW so that F remains constant. This results in a perturbation of the potential amplitude $\delta A = 0.05A$. Then, the integrated response function of $\phi(\theta)$ at time $t \geq 0$ due to the perturbation $-\delta A$ applied at time 0 is given by

$$\chi_{QV}(t) = \frac{\langle \phi(\theta_t) \rangle_{\delta A} - \langle \phi(\theta_t) \rangle_0}{-\delta A}, \tag{9}$$

where $\langle ... \rangle_{\delta A}$ and $\langle ... \rangle_0$ denote the ensemble averages of the perturbed $\theta_{t,\delta A}$ and unperturbed θ_t trajectories, respectively. In order to decrease the statistical errors in comparison of the terms in equation (9), for a given perturbed trajectory $\theta_{t,\delta A}$ we look for as many unperturbed ones θ_t as possible starting at time t^* such that $\phi(\theta_{t^*}) = \phi(\theta_{0,\delta A})$. Then we redefine t^* as $t = 0$ in equation (9), as depicted in figure 2(a). The unperturbed trajectories found in this way allow us to define a subensemble over which the average $\langle ... \rangle_0$ is computed. On the other hand, the average $\langle ... \rangle_{\delta A}$ is performed over 500 independent realizations of δA that are enough for a fair determination of the integrated response. The resulting curve $\chi_{QV}(t)$ and its corresponding error bars $\pm\sigma_\chi(t)$ as functions of the integration time t starting at the instant of the application of the step perturbation are shown in figures 2(c) and 2(d).
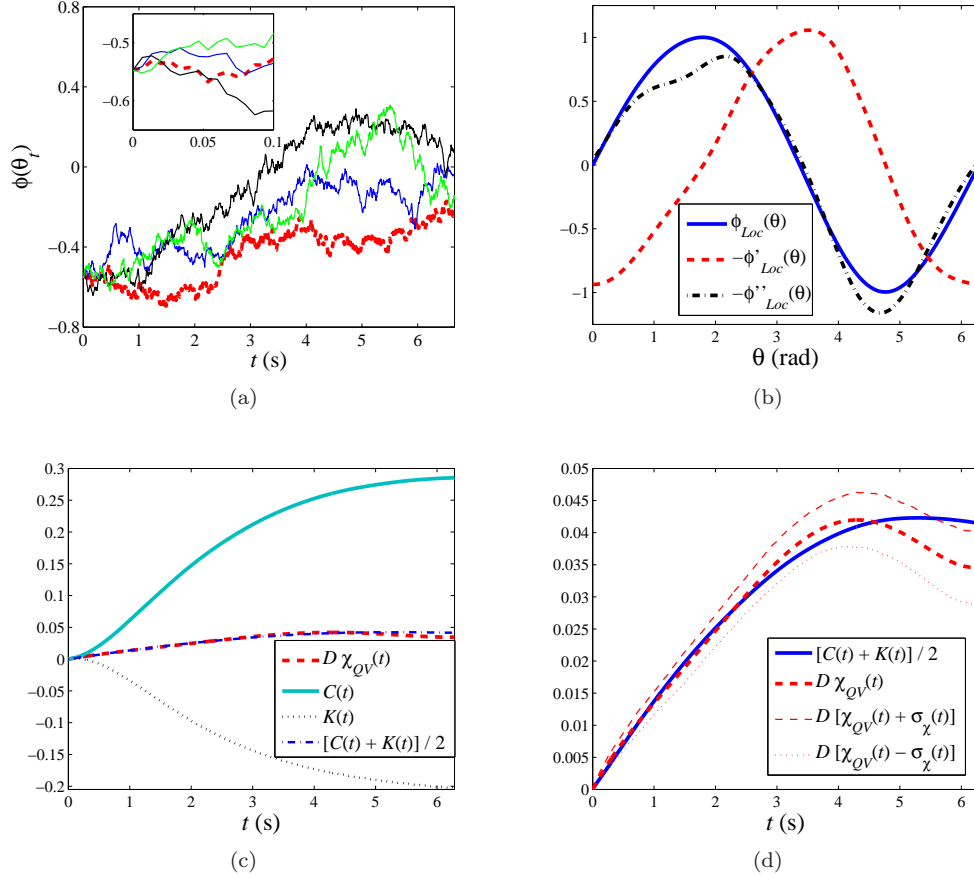
Figure 2: (a) Examples of a perturbed trajectory (red thick dashed line) and three unperturbed steady-state trajectories (thin solid lines) used to compute the integrated response function given by equation (9). Inset: expanded view at short time. The unperturbed trajectories are chosen to start at the same value as the perturbed one. (b) Potential profile $\phi(\theta)$ locally fitted as a third-order polynomial $\phi_{Loc}(\theta)$ around each value of θ. Their derivatives are computed from $\phi_{Loc}(\theta)$. (c) Integrated linear response function $\chi_{QV}(t)$, entropic $C(t)$ and frenetic $K(t)$ terms and the corresponding indirect measurement of the response $[C(t) + K(t)]/2$ for $Q = \phi(\theta)$, $h = -\delta A$ and $V = \phi(\theta)$, as functions of the integration time t. (d) Expanded view of (c).

7

4.2 Indirect measurement of the linear response function

The same response information can be obtained *indirectly* from correlation measurements of the unperturbed non-equilibrium steady-state fluctuations ($\delta A = 0$) of θ_t when properly using equation (5). For the Langevin dynamics of θ described by equation (8) the analytical expression of the generator L is

$$L = (F - A\phi'(\theta))\partial_\theta + D\partial_\theta^2. \tag{10}$$

Hence, in this case equation (5) reads

$$D\chi_{QV}(t) = \frac{C(t) + K(t)}{2}, \tag{11}$$

where the entropic and frenetic terms are

$$C(t) = \langle\phi(\theta_t)\phi(\theta_t)\rangle_0 - \langle\phi(\theta_0)\phi(\theta_t)\rangle_0, \tag{12}$$

$$K(t) = -\int_0^t ds\langle[D\phi''(\theta_s) + (F - A\phi'(\theta_s))\phi'(\theta_s)]\phi(\theta_t)\rangle_0, \tag{13}$$

respectively. At this point it is clear that we need to know the potential profile $\phi(\theta)$ for the indirect method. The integrand of equation (13) involves the instantaneous values of $\phi(\theta)$ and its derivatives $\phi'(\theta)$ and $\phi''(\theta)$. In order to take into account the non-sinusoidal distortion of the potential profile, we perform a local polynomial fit ϕ_{Loc} of ϕ around each value of $\theta \in [0, 2\pi)$. Then the instantaneous value of the observable $\phi(\theta_t)$ at time t is approximated by $\phi_{Loc}(\theta_t)$ either for an unperturbed or a perturbed trajectory. The local polynomial approximation ϕ_{Loc} and its derivatives ϕ'_{Loc}, ϕ''_{Loc} are plotted in figure 2(b) showing the non-sinusoidal distortion.

The resulting curves $C(t)$ and $K(t)$ as functions of the integration time t are plotted in figure 2(c). At thermal equilibrium ($F = 0$) one should find that $C(t) = K(t)$ for all $t \geq 0$ because of the time reversibility and stationarity of the two-time correlations leading to the equilibrium fluctuation-dissipation relation $D\chi_{QV}(t) = C(t)$. On the other hand, in the present case $K(t)$ reaches negative values of the same order of magnitude as the positive values of $C(t)$. This reflects the experimental conditions far from thermal equilibrium of the system. The curve for $K(t)$ represents the first experimental result concerning the direct measurement of the dynamical activity along a trajectory [13, 14, 15]. The average of these two quantities $[C(t)+K(t)]/2$ is one order of magnitude smaller. This average, which is an indirect measurement of the integrated response function according to equation (11), agrees very well with the direct measurement of χ_{QV} within the experimental error bars, as shown in figure 2(d). All is consistent with the results of [16], see [6, 13], but the experimental approach here is quite different. The experimental verification of previous equivalent generalized fluctuation-dissipation relations for the same experimental system as the one studied here [16, 18, 20] involves the local mean velocity of the particle (*i.e.* the ratio between the steady-state current and the probability density). Here we measure directly explicit correlation functions $C(t)$ and $K(t)$ without recourse to and indeed without need for the expression for the stationary distribution. Note that the experimental density profile $\rho(\theta)$ (and not its analytical expression) is used in practice only for calibration purposes [16, 17] to determine the experimental parameters A and F. However, once these parameters are known the data analysis necessary to compute $C(t)$ and $K(t)$ completely relies on the dynamics, i.e. the measurement of the time series θ_t. Thus, this procedure is suitable for the study of the linear response of more complex Markovian non-equilibrium situations (*e.g.* multiple degrees of freedom, non-stationary states, several thermal baths) where local mean velocities are not easily measurable in experiments.

4.3 Discussion

We remark that for this kind of micron-sized system the relation (5) actually represents a feasible indirect method to access the linear response regime far from thermal equilibrium. This is because all the parameters of the unperturbed dynamics are known a priori or can be determined in situ without any external perturbation of the non-equilibrium state. On the other hand, the direct measurement of the linear response function exhibits a number of technical difficulties in practice. First, a vanishingly small Heaviside perturbation $-hV(q)$ to the initially unperturbed potential $U(q)$ is ideally required. Otherwise spurious effects quickly bias the measurement of χ_{QV}, specially when the system is strongly non-linear. Second, one requires an extremely large number of independent realizations of h to resolve χ_{QV} as the perturbation $-hV(q)$ must be chosen very weak, typically smaller than the thermal fluctuations of the energy injected by the environment. This is evident on the results of the direct measurement of χ_{QV} for the colloidal particle, see figure 2(d). For integration times $t \lesssim 3$ s the agreement between $D\chi_{QV}(t)$ and $[C(t) + K(t)]/2$ is excellent. Then, for $t \gtrsim 3$ s the finite sampling leads to deviations between the two methods and increasingly large error bars for the direct measurement of χ_{QV}. These drawbacks are skipped when implementing the indirect method measuring the unperturbed quantity $[C(t) + K(t)]/2$. In addition, for a steady state like the one experimentally studied here one can improve dramatically the statistics by performing an additional time average over a window $[0, t_{max}]$ [1] : $\bar{C}(t) = \int_0^{t_{max}} C(t+u)\mathrm{d}u/t_{max}$, $\bar{K}(t) = \int_0^{t_{max}} K(t+u)\mathrm{d}u/t_{max}$, as actually done for the curves C, K and $(C+K)/2$ in figures 2(c) and 2(d). However, one must be careful when performing the time average. This is because the value of t_{max} may affect the resulting values of $[C(t) + K(t)]/2$ as t increases, specially for correlation functions involving strongly fluctuating quantities such as velocities, as recently discussed in [20]. For the curves shown in figures 2(c) and 2(d) we verified that their shapes are not significantly influenced by t_{max}.

4.4 Application example

Finally, we illustrate the usefulness of the indirect measurement of the linear response function to study the temporal behavior of the mean potential energy of the particle $\langle U(\theta_t)\rangle_h$ under small external perturbations h_s more intricate than a simple Heaviside function. This is done with the same unperturbed experimental data used in subsection 4.2 without carrying out the different physical realizations of h_s. We concentrate on a sinusoidal perturbation starting at time $s = 0$

$$h_s = h_0 \sin 2\pi f_0 s. \tag{14}$$

either to the phase or to the amplitude of the potential around the steady state. First, we consider the case of a small phase perturbation $\alpha_s = \alpha_0 \sin 2\pi f_0 s$ with $\alpha_0 \ll 1$: $A\phi(\theta) \to A\phi(\theta + \alpha_s) \approx A\phi(\theta) + A\phi'(\theta)\alpha_s$ so that $h_0 = -A\alpha_0$ in equation (14) and $V = \phi'(\theta)$. One must compute first the integrated response function of $Q = \phi(\theta)$ given by $[C(t) + K(t)]/(2D)$ by inserting the right V and Q in equations (6) and (7). The resulting curves $C(t)$, $K(t)$ and $[C(t) + K(t)]/(2D)$ are plotted in figure 3(a). Next, using equation (2) the experimental impulse response function $[\partial_t C(t-s) + \partial_t K(t-s)]/(2D)$ must be convolved with h_s given by equation (14). In this way one finds that the mean potential energy of the particle oscillates around the non-equilibrium steady state value $\langle U(\theta)\rangle_0 = -4.7k_B T$ as shown by the dashed blue line in figure 3(b) for $\alpha_0 = 0.05$ rad and $f_0 = 1$ Hz. The oscillations exhibit a delay time ($\Delta t \approx 0.23$ s) with respect to α_s and a slow transient (~ 15 s) corresponding to the decay of the non-equilibrium stationary correlations. As t increases the oscillations settle around $\langle U(\theta)\rangle_0$ with a constant amplitude $\Delta U \approx 0.2k_B T$. Now, we consider a sinusoidal time-dependent perturbation to the potential

---

[1] The only restriction in the choice of t_{max} is that the ensemble of averaging intervals $[\theta_0, \theta_{t_{max}}]$ must cover the whole circle to sample correctly the steady state.
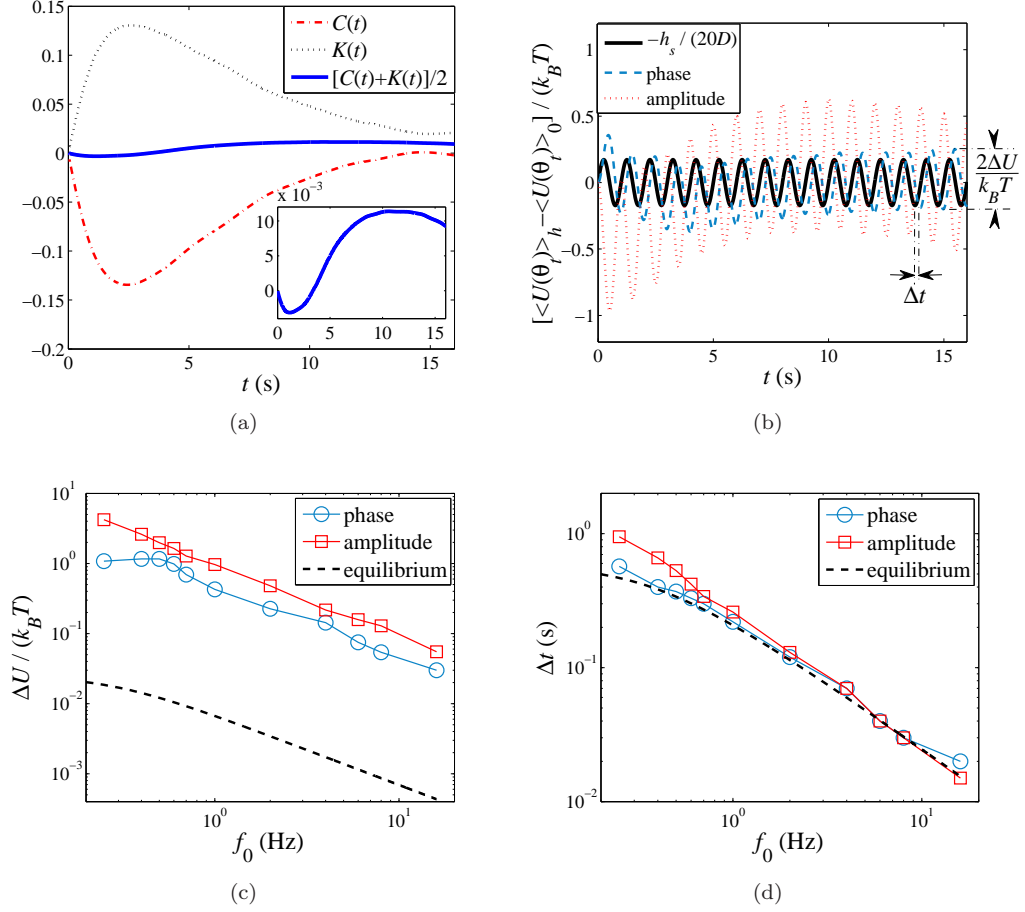
Figure 3: a) Integrated response function of the observable $Q = \phi(\theta)$ for a small perturbation of the potential phase as a function of the integration time t. Inset: expanded view of $[C(t) + K(t)]/2$. (b) Sinusoidal time-dependent perturbation $-h_s$ (solid black line) of the static potential $A\phi$. Resulting mean potential energy of the Brownian particle for a phase perturbation (dashed blue line) and an amplitude perturbation (dotted red line) for $-h_0/A = 0.05$ and $f_0 = 1$ Hz. (c) Asymptotic values of oscillation amplitude of the potential energy and (d) the delay time with respect to $-h_s$ for each kind of perturbation. The black dashed lines represent the values that would be obtained around thermal equilibrium ($F = 0$), given by equations (17) and (18).

amplitude: $\delta A_s = \delta A_0 \sin 2\pi f_0 s$ with the same strength ($-h_0/A = 0.05$) and frequency as before. In this case $h_0 = -\delta A_0$ and $V = \phi(\theta)$. Following the same procedure with $[C+K]/(2D)$ shown in figure 2(d), one finds a different qualitative behavior of $\langle U(\theta_t) \rangle_h$, as depicted by the dotted red line in figure 3(b). At the beginning the mean potential energy responds in the opposite direction to δA_s. Then, as t becomes larger than the slow non-equilibrium transient $\langle U(\theta) \rangle_h$ oscillates around $\langle U(\theta) \rangle_0$ with a constant amplitude $\Delta U \approx 0.5 k_B T$ and a delay time $\Delta t \approx 0.26$ s. For both types of perturbations one can write the asymptotic dependence of $\langle U(\theta_t) \rangle_h$ on $t \gtrsim 15$ s as

$$\langle U(\theta_t) \rangle_h = \langle U(\theta_t) \rangle_0 \pm \Delta U \sin[2\pi f_0(t - \Delta t)], \tag{15}$$

where the positive and negative signs stand for the phase and amplitude perturbations, respectively. The values of ΔU and Δt depend on the frequency f_0. In figures 3(c) and 3(d) we show this dependence. We now compare these far-from-equilibrium results with those that would be obtained when applying h_s around thermal equilibrium ($F = 0$). In such a case the particle motion is tightly confined to the harmonic part of the potential around the minimum $\theta_m = 3\pi/2$: $\phi(\theta) \approx -1 + (\theta - \theta_m)^2/2$. After some algebra using this approximation one finds the expression for $\langle U(\theta_t) \rangle_h$ when perturbing thermal equilibrium

$$\begin{aligned}\langle U(\theta_t) \rangle_h &= \langle U(\theta_t) \rangle_0 \pm \Delta U \{\sin[2\pi f_0(t - \Delta t)] + \\ &\quad e^{-2At} \sin 2\pi f_0 \Delta t\},\end{aligned} \tag{16}$$

where $\langle U(\theta_t) \rangle_0 = -68.3 k_B T$ and

$$\Delta U = -\frac{h_0}{A} \frac{k_B T}{2(1 + \pi^2 f_0^2/A^2)^{1/2}}, \tag{17}$$

$$\Delta t = \frac{1}{2\pi f_0} \arctan\left(\frac{\pi f_0}{A}\right), \tag{18}$$

either for a phase (positive sign) or an amplitude (negative sign) perturbation. Note that for $t \gg (2A)^{-1}$, equation (16) exhibits the same qualitative behavior as (15). We plot the curves given by eqsuations (17) and (18) in figures 3(c) and 3(d), respectively, for the same values of the parameters h_0 and A as before. Unlike the behavior close to equilibrium, the oscillation amplitude ΔU strongly depends on the perturbed parameter around the non-equilibrum steady state: it is more sensitive to amplitude perturbations than to phase perturbations. In addition, the far-from-equilibrium values are two orders of magnitude larger than that given by equation (17). By contrast, the delay time Δt is not significantly affected by the far-from-equilibrium nature of the system. It is almost independent of F and of the type of perturbation and it converges to equation (18) as f_0 increases.

5   Concluding remarks

We have experimentally studied the non-equilibrium linear response of the potential energy of a Brownian particle in a toroidal optical trap. We gain insight into the application of the fluctuation-dissipation relations far from thermal equilibrium in this non-linear system with a single relevant degree of freedom. In particular, we show that the entropic-frenetic approach is appropriate and feasible for the study of the linear response of non-equilibrium micron-sized systems with a small number of degrees of freedom immersed in simple fluids. Non-trivial linear response information can be obtained from purely unperturbed measurements of the non-equilibrium fluctuations provided that the parameters describing the dynamics are known. Our

experiment reveals that the indirect determination of the linear response function is less time-consuming, more accurate and more flexible than the direct perturbation of the non-equilibrium system. Similar ideas are expected to be applicable to more complex micron-sized systems such as atomic-force microscopy experiments and ensembles of colloidal particles in simple non-equilibrium conditions where local mean velocities are difficult to measure.

References

[1] H. B. Callen and T. A. Welton, 1951 Phys. Rev. **83**, 34.

[2] G. S. Agarwal, 1972 Z. Phys. **252**, 25.

[3] T. Harada and S.-I. Sasa, 2005 Phys. Rev. Lett. **95**, 130602.

[4] E. Lippiello, F. Corberi, and M. Zannetti, 2005 Phys. Rev. E **71**, 036104.

[5] T. Speck and U. Seifert, 2006 Europhys. Lett. **74**, 391.

[6] R. Chetrite, G. Falkovich, and K. Gawedzki, J. Stat. Mech. (2008) P08005.

[7] K. Martens, E. Bertin, and M. Droz, 2009 Phys. Rev. Lett. **103**, 260602.

[8] A. Puglisi and D. Villamaina, 2009 EPL **88**, 30004.

[9] D. Villamaina, A. Baldassarri, A. Puglisi, and A. Vulpiani, J. Stat. Mech. (2009) P07024.

[10] J. Prost, J.-F. Joanny, and J. M. R. Parrondo, 2009 Phys. Rev. Lett. **103**, 090601.

[11] U. Seifert and T. Speck, 2010 EPL **89**, 10007.

[12] R. Chetrite, and G. Gawedzki, 2009 J. Stat. Phys. **137**, 890.

[13] M. Baiesi, C. Maes and B. Wynants, 2009 Phys. Rev. Lett. **103**, 010602.

[14] M. Baiesi, C. Maes and B. Wynants, 2009 J. Stat.Phys. **137**, 1094.

[15] M. Baiesi, E. Boksenbojm, C. Maes and B.Wynants, 2010 J. Stat. Phys. **139**, 492.

[16] J. R. Gomez-Solano, A. Petrosyan, S. Ciliberto, R. Chetrite, and K. Gawedzki, 2009 Phys. Rev. Lett. **103**, 040601.

[17] V. Blickle, T. Speck, U. Seifert, and C. Bechinger, 2007 Phys. Rev. E **75**, 060101(R).

[18] V. Blickle, T. Speck, C. Lutz, U. Seifert, and C. Bechinger, 2007 Phys. Rev. Lett. **98**, 210601.

[19] V. Blickle, J. Mehl, and C. Bechinger, 2009 Phys. Rev. E **79**, 060104(R).

[20] J. Mehl, V. Blickle, U. Seifert, and C. Bechinger, 2010 Phys. Rev. E **82**, 032401.

[21] C. Maes, K. Netocny, and B. Wynants, 2008 Physica A **387**, 2675.